Int. J. Solids Structures Vol. 25, No. 2, pp. 151–165, 1989
Printed in Great Britain.

0020–7683/89 $3.00 + .00

ANALYSIS OF SINGULAR CYLINDRICAL SHELLS BY *p*-VERSION OF FEM

KWANG S. WOO and PRODYOT K. BASU
Department of Civil Engineering, Vanderbilt University, Nashville, TN 37235, U.S.A.

(*Received* 23 *December* 1987; *in revised form* 6 *June* 1988)

Abstract—A new hierarchic *p*-version cylindrical shell element based on exact mapping is presented. Its rigid-body modes, round-off error, and convergence characteristics are investigated. Its performance in the presence of singularities is demonstrated with the help of three test problems, namely pinched cylinder problem, Lockheed test problem 2, and cracked cylinder problem.

1. INTRODUCTION

Structural shells are widely used in a broad spectrum of industries, e.g. aerospace, automotive, power generation, railroad, ship building, and chemical. Very often the usage is characterized by irregularities in the form of discontinuities, complex loading and support conditions over the surface and at the edges.

In the design of such shells it is necessary to account for the aforementioned irregularities, which may, sometimes, become the source of singularities in the stress field and hence the potential seat for crack initiation and propagation, affecting the fatigue life of the shell under cyclic loading conditions.

The sources of singularities can be classified under three headings (Basu and Peano, 1981; Lukasiewicz, 1976).

(1) Geometric: re-entrant corners, cracks, cutouts with sharp corners, discontinuities in curvature and thickness, presence of stiffeners, mixed boundary conditions, and the like.
(2) Loading: concentrated sources over the surface and at the edges, line sources over the surface, and sudden changes in the intensity of the external sources.
(3) Material: sudden changes in material properties, as in the case of laminated materials.

As the stress gradients in the vicinity of a singular point are very steep, the *p*-version of the finite element method is expected to perform very well for modeling such problems (Basu *et al.*, 1977). The main objective of this paper is to develop cylindrical shell elements based on the *p*-version of FEM and to study their performance in the case of cylindrical shells with polygonal cutouts and cracks, as well as in the presence of concentrated loads.

The *h*-version, which is normally based upon Lagrange polynomial interpolation through evenly distributed nodal points, is less reliable at the boundaries than in the interior regions. However in the *p*-version, the roots of Legendre polynomials, unlike the roots of Lagrange polynomials, are not evenly distributed in the interval $-1 < x < 1$ but rather are closely grouped near the endpoints (Basu, 1986). Thus at the end points, very steep strain gradients can be modeled effectively when integrals of Legendre polynomials are used to create the basis functions. These polynomials are able to oscillate with increased frequency near the endpoints and thus are better suited for approximating singular behavior which occurs at these points than with uniform *h*-version meshes. In modeling the singular behavior caused by sharp cracks, one could however use a quarter-point element in the context of the *p*-version, to represent the strength of singularity exactly.

It has been demonstrated by numerical experimentation and analytical reasoning that the rate of convergence of the *p*-version is twice the rate for the *h*-version when severe corner singularities are present, and the number of degrees of freedom is increased by uniform or quasi-uniform mesh refinement (Basu and Peano, 1981; Cheng, 1986; Peano

et al., 1978). Moreover, the superior performance of the *p*-version in modeling transversely loaded plates with polygonal cutouts, and the classical rhombic plate problem is evidenced in Basu *et al.* (1977) and Basu and Peano (1981).

In the conventional *h*-version, there are three distinct approaches to the finite element representation of thin shell structures (Ashwell and Gallagher, 1976): (i) in "faceted" form with flat elements; (ii) by means of degenerated three-dimensional (solid) elements; and (iii) with elements formulated on the basis of curved shell theory. The shortcomings and associated difficulties of "faceted" elements are well known.

Corresponding to the six displacement components of a cylindrical shell, that is u, v, w, θ_x, θ_y, θ_z, there should be six rigid-body modes, and hence the element stiffness matrix should have six zero eigenvalues related to these modes. Different schemes have been put forward by Cantin (1970) and others for the problem of ensuring rigid-body displacements in shell elements. In the development of a general shell element of arbitrary thickness and geometry that reproduced the rigid-body motions exactly, Hansen and Heppler (1985) used strain–displacement relationships of the Mindlin type, based on a curvilinear coordinate system.

2. HIERARCHICAL SHELL ELEMENTS

2.1. *Integrals of Legendre shape functions*

The shape functions used in this study are based on the *integrals of Legendre polynomials*. The lowest order shape functions ($p = 1$) being expressed as

$$N_k = \frac{(1+\xi\xi_k)(1+\eta\eta_k)}{4} \tag{1}$$

in which subscript "k" refers to the four vertex nodes of the standard element, as shown in Fig. 1. For each higher p-level four more edge shape functions (Basu and Peano, 1981), are required to be added as

$$\begin{aligned} &(1\pm\eta)F_p(\xi) \quad \text{for edges } \eta = \pm 1 \\ &(1\pm\xi)F_p(\eta) \quad \text{for edges } \xi = \pm 1 \end{aligned} \tag{2}$$

where

$$F_p(x) = \sqrt{\frac{(2p-1)}{2}} \int_{-1}^{x} P_{p-1}(t)\, dt \tag{3}$$

in which $P_n(t)$ is the Legendre polynomial defined by the Rodrigues formula

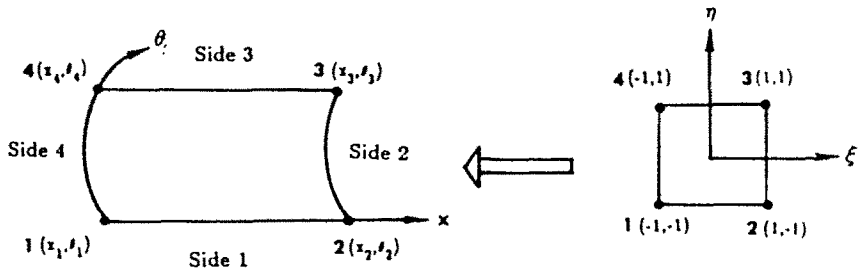

Fig. 1. Blend mapping from standard domain to real domain.

$$P_n(t) = \frac{1}{2^n n!} \frac{d^n}{dt^n} (t^2 - 1)^n. \tag{4}$$

The completeness requirement is satisfied by introducing internal nodes for $p \geqslant 4$ as $F_i(\xi)F_j(\eta)$ with the requirement that $i+j = p$ and that $i, j \geqslant 2$ (Basu and Peano, 1981). In the case of two-dimensional problems, these shape functions are not exactly orthogonal in energy norm, unlike the case of one-dimensional problems, but will be nearly so and hence are expected to give well-conditioned stiffness matrices.

2.2. *Blend mapping*

In order to conform better to curved geometries and thus reduce the discretization error, curved finite elements have been widely used in recent years. The most well known of such elements are the parametric (iso- or sub-) family of elements.

For mathematical convenience, in general, the shape functions are defined on standard domains (e.g. triangles, squares, cubes, etc.) and are mapped into the real domain by suitable coordinate transformations. The most commonly used mappings are linear and quadratic parametric mappings which have served the h-version well. This is because, in general, the mapping does not introduce large distortions in the h-version, and all piecewise smooth boundaries can be approximated by a sufficient number of piecewise quadratic polynomials.

In the p-version, the size of the elements is usually large and hence the probability of distortions is more, especially if higher order parametric mapping is used, unless the boundary of an element is represented by a polynomial in the parametric form. In the case of non-polynomial boundaries, like circles and ellipses, parametric mapping may not work at all.

In the case of the proposed element, only the four corners of a quadrilateral element will be referred to in mapping from the standard to the real domain. It is therefore necessary to find the mapping function which will exactly map the standard element to the sides of the element including the four corner nodes by making use of the exact geometric parameters of the curved boundaries (Fig. 1). This can be achieved by constructing blend mapping functions (Gordon, 1971). As a special case, the mapping function for an element bounded by lines x = const. and θ = const. can be expressed as

$$x = \sum_{k=1}^{4} M_k(\xi, \eta) x_k$$
$$\theta = \sum_{k=1}^{4} M_k(\xi, \eta) \theta_k \tag{5}$$

where

$$M_k(\xi, \eta) = \tfrac{1}{4}(1 + \xi\xi_k)(1 + \eta\eta_k).$$

2.3. *Formulation of element stiffness matrix*

As per standard displacement formulation, the element stiffness matrix will be expressed as

$$[\mathbf{K}^e] \pm \int\int [\mathbf{B}]^T [\mathbf{D}][\mathbf{B}] \, dA. \tag{6}$$

2.3.1. *Strain matrix* [B]. The following strain–displacement relationships are used in evaluating the stiffness matrix

$$\begin{bmatrix} \varepsilon_x \\ \varepsilon_\theta \\ \varepsilon_{x\theta} \\ \chi_x \\ \chi_\theta \\ \chi_{x\theta} \\ \phi_x \\ \phi_\theta \end{bmatrix} = \begin{bmatrix} \frac{\partial}{\partial x} & 0 & 0 & 0 & 0 \\ 0 & \frac{\partial}{R\partial\theta} & \frac{1}{R} & 0 & 0 \\ \frac{\partial}{R\partial\theta} & \frac{\partial}{\partial x} & 0 & 0 & 0 \\ 0 & 0 & 0 & \frac{\partial}{\partial x} & 0 \\ 0 & 0 & 0 & 0 & \frac{\partial}{R\partial\theta} \\ 0 & 0 & 0 & \frac{\partial}{R\partial\theta} & \frac{\partial}{\partial x} \\ 0 & 0 & \frac{\partial}{\partial x} & 1 & 0 \\ 0 & \frac{-1}{R} & \frac{\partial}{R\partial\theta} & 0 & 1 \end{bmatrix} \begin{bmatrix} u \\ v \\ w \\ \theta_x \\ \theta_y \end{bmatrix}$$

or

$$\varepsilon = \mathbf{B}\delta^e. \tag{7}$$

2.3.2. *Elasticity matrix* [**D**]. The constitutive relationships for an elastic isotropic material, in the absence of initial stresses and strains, can be expressed as

$$\begin{bmatrix} N_x \\ N_\theta \\ N_{x\theta} \\ M_x \\ M_\theta \\ M_{x\theta} \\ Q_x \\ Q_\theta \end{bmatrix} = \begin{bmatrix} K_1 & K_2 & 0 & 0 & 0 & 0 & 0 & 0 \\ K_2 & K_1 & 0 & 0 & 0 & 0 & 0 & 0 \\ 0 & 0 & K_3 & 0 & 0 & 0 & 0 & 0 \\ 0 & 0 & 0 & D_1 & D_2 & 0 & 0 & 0 \\ 0 & 0 & 0 & D_2 & D_1 & 0 & 0 & 0 \\ 0 & 0 & 0 & 0 & 0 & D_3 & 0 & 0 \\ 0 & 0 & 0 & 0 & 0 & 0 & S_1 & 0 \\ 0 & 0 & 0 & 0 & 0 & 0 & 0 & S_1 \end{bmatrix} \begin{bmatrix} \varepsilon_x \\ \varepsilon_\theta \\ \varepsilon_{x\theta} \\ \chi_x \\ \chi_\theta \\ \chi_{x\theta} \\ \phi_x \\ \phi_\theta \end{bmatrix}$$

or

$$\sigma = \mathbf{D}\varepsilon \tag{8}$$

in which **D** is the constitutive matrix, with

$$K_1 = \frac{Et}{1-\nu^2}, \qquad K_2 = \nu K_1$$

$$K_3 = \tfrac{1}{2}(1-\nu)K_1, \quad D_1 = \frac{Et^3}{12(1-\nu^2)}$$

$$D_2 = \nu D_1, \qquad D_3 = \frac{1-\nu}{2} D_1$$

$$S_1 = \frac{Et}{2(1+\nu)\alpha}; \qquad \alpha = 6/5.$$

The N^e, M^e and Q^e represent the membrane, flexural, and transverse shear stress resultants

per unit length of the shell. It may be noted that eqns (7) and (8) include the effect of transverse shear deformations, and the inverse of the factor α is the so-called shear correction factor.

After the shape functions are substituted into matrix [**B**], the element stiffness matrix can be evaluated from eqn (6). A typical submatrix of $[\mathbf{K}^e]$ linking nodes i and j can then be evaluated with the expression

$$[\mathbf{K}_{ij}^e] = \int\int [\mathbf{B}_i]^T[\mathbf{D}][\mathbf{B}_j]\, dA$$

in which

$$dA = R\, d\theta\, dx = R \det \mathbf{J}\, d\xi\, d\eta$$

$$\det \mathbf{J} = \text{determinant of the Jacobian matrix.}$$

3. COMPUTER IMPLEMENTATION

In the program, SHLPV, developed for this study, up to a maximum of 12×12 Gauss point rules for numerical quadrature have been built in. The susceptibility of a matrix to round-off errors in the solution of a simultaneous equation is characterized by the condition number (CN). It can be shown that the maximum number of digits lost in numerical operations involving a given matrix is not greater than log (CN).

As a result, the shape functions that perform better numerically are the ones that will result in a stiffness matrix that has a smaller condition number. In general, the stiffness matrix [K] will be ideally well-conditioned if CN is close to one, and ill-conditioned when CN is significantly greater than one. In order to calculate the CN of the stiffness matrix one has to extract the largest and smallest eigenvalues of the following equation. In this study the Jacobi method is adopted for this purpose

$$([K] - \lambda[I])\{u\} = 0. \tag{9}$$

The condition number can then be defined as $CN = |\lambda_{max}|/|\lambda_{min}|$ and the loss of significant digits will be log (CN), approximately.

In the case of shell elements with a central angle of 90°, a radius of 4.953 in., a Poisson's ratio of 0.3125, a Young's modulus of 10.5×10^6 and R/t ratios of 16.5, 52.69, and 319.96, the variation of the loss of significant digits with p-level are shown in Fig. 2. It can be seen that the maximum number of digits lost lies between 2 for p = 1–5, 6, or 7 for a thick, thin and very thin shell when $p = 8$. It may be noted that for $p \geqslant 3$, the number of digits lost remains virtually unchanged.

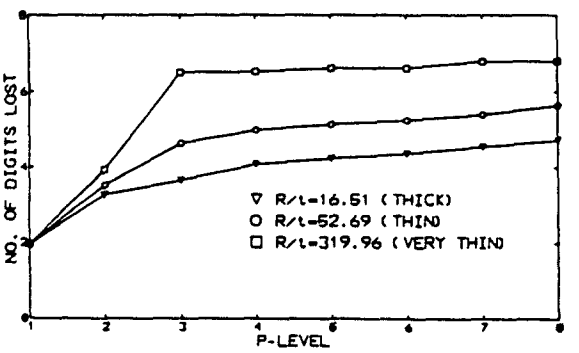

Fig. 2. Condition number of cylindrical shell element (R = 4.953 in., ν = 0.3125, $E = 10.5 \times 10^6$, central angle = 90°).

Table 1. Eigenvalues of cylindrical thin shell element when $p = 8$

	Eigenvalue
λ_1	0.77594E−10
λ_2	0.56157E−09
λ_3	0.36391E−09
λ_4	0.42362E−02
λ_5	0.79867E−04
λ_6	0.18612E−09
λ_7	0.32015E+02
λ_8	0.35772E+02
λ_9	0.39425E+02
λ_{max}	0.13918E+08

The first nine eigenvalues for a cylindrical shell element which is a quarter-cylinder with $R = 4.953$ in., $t = 0.094$ in. are shown in Table 1. It may be noted that the first six eigenvalues are small enough, compared to the remaining eigenvalues, to be treated as zero and hence the proposed element satisfies the rigid-body motion requirements.

4. NUMERICAL RESULTS

4.1. *Pinched cylindrical shell*

Two problems are considered, one a thin shell with $R/t = 53$, and the other a very thin shell with $R/t = 320$. The first shell was analyzed by Bogner *et al.* (1967). Recently this problem was solved by Hansen and Heppler (1985) and Carpenter *et al.* (1986). It has a radius of 4.953 in., a thickness of 0.094 in., and a pinch load of 100 lb. The second shell has the same radius as the first but its thickness is taken as 0.01548 in., and its pinch load is 0.1 lb. For both shells, the Young's modulus is taken as 10.5×10^6 psi and Poisson's ratio as 0.3125. Because of the symmetry only one octant of the shell, as shown in Fig. 3, is considered.

In the case of the first shell the radial deflection under the point load based on thin shell equations is 0.1084 in. (Timoshenko and Woinowsky-Krieger, 1959). An ABAQUS

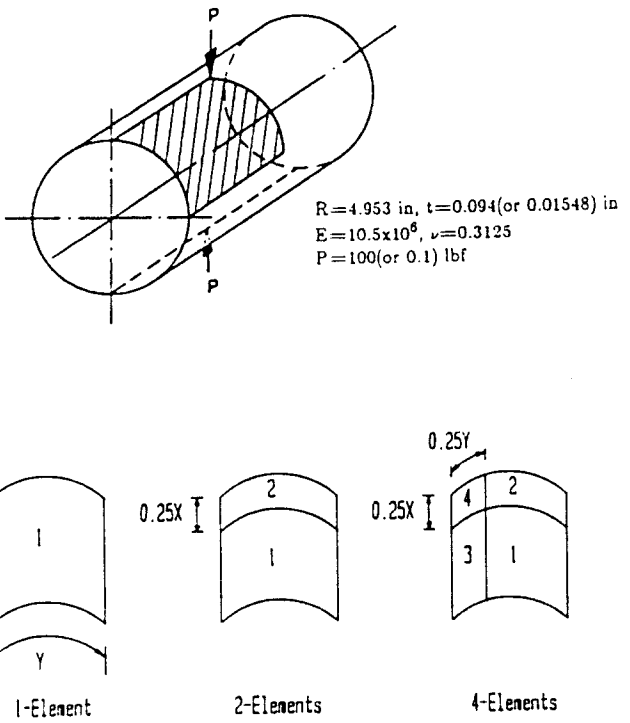

Fig. 3. An octant of the pinched cylinder problem and mesh refinement.

Table 2. Deflection (in.) under point load for thin pinched cylinder problem

Mesh	Cantin (1970)	Ashwell and Sabir (1972)	Thomas and Gallagher (1975)	Bogner *et al.* (1967)	Mesh	Cantin and Clough (1968)
1 × 1		0.104(20)	0.0048(19)	0.0025(48)		
1 × 2				0.0802(72)	1 × 3	0.0297(48)
1 × 4		0.1106(50)	0.1107(67)	0.1087(120)	1 × 5	0.0769(72)
1 × 8			0.1119(131)		1 × 7	0.0987(96)
2 × 2	0.0931(54)	0.1103(45)		0.0808(108)	1 × 9	0.1057(120)
4 × 4	0.1126(150)	0.1129(125)			2 × 9	0.1073(180)
6 × 6	0.1137(294)	0.1135(245)			3 × 49	0.1128(1200)
8 × 8	0.1139(486)	0.1137(405)				
10 × 10	0.1139(726)	0.1137(605)				
5 × 5	0.1135(390) ABAQUS S8R element					
10 × 10	0.1115(540) ABAQUS S4R element					
1 × 1	0.1126(110) $p = 8$ by p-version					
2 × 2	0.1134(125) $p = 5$ by p-version					

Figures in parentheses give *NDOF*.

(1985) solution based on a [5 × 5] mesh of S8R elements is found to be 0.1135 in. and with a [10 × 10] mesh of S4R elements the value is 0.1115 in. The results for this problem published by different authors and those by the p-version (i.e. present study) are shown in Table 2. The importance of rigid-body modes is evident from the results of Cantin and Clough (1968) with a [3 × 49] mesh. A deflection of 0.1128 in. was obtained by them when the rigid-body modes were included and the value was 0.05583 in. when the rigid-body modes were excluded. The p-version result is 0.1126 in. with a single eighth-order element.

Table 3 shows the deflection (in.) under the pinch load for the very thin pinched cylinder problem. The best available analytical result is 0.02439 in. (Ashwell and Gallagher, 1976). An ABAQUS (1985) solution based on a [5 × 5] mesh of S8R elements is found to be 0.02453 in. and with a [10 × 10] mesh of S4R elements 0.02405 in. The p-version result with a single eighth-order element ($NDOF = 110$) is 0.024413 in.

The convergence characteristics of maximum deflection and total potential energy for a single element model of the thin cylinder, as the p-level is increased from four to nine, are shown in Figs 4 and 5. With just one element the results appear to converge at a p-level of 6.

The effect of mesh refinement, keeping the p-level fixed at 5, is shown in Table 4. The meshes used for this purpose are graded towards the point load, as shown in Fig. 3. With one element and $p = 9$, the maximum deflection is 0.1130 in. Whereas in Table 4 the graded four-element model with $p = 5$ gives a value of 0.1134 in. Therefore, a graded mesh with a sufficiently high p-level leads to better results with somewhat fewer degrees of freedom.

To achieve the same degree of accuracy, the CPU time requirements of the p-version solution with one element was found to be 13.86 s as compared to 29.43 s with ABAQUS

Table 3. Deflection (in.) under point load for very thin pinched cylinder problem

Mesh	Ashwell and Sabir (1972)	Thomas and Gallagher (1975)	Cantin and Clough (1968)	Sabir and Lock (1972)
1 × 1	0.2301(20)	0.00003(19)	0.00001(24)	0.00001(20)
1 × 2		0.01582(35)		
1 × 4	0.02403(50)	0.02327(67)	0.00074(64)	0.00063(50)
1 × 6		0.02440(99)		
1 × 8	0.02406(90)	0.02467(131)	0.00700(108)	0.00691(90)
2 × 8	0.02414(135)		0.00699(162)	0.00694(135)
3 × 8	0.02418(180)		0.00699(216)	0.00696(180)
8 × 8	0.02431(405)		0.00708(486)	0.00706(405)
5 × 5	0.02453(390) ABAQUS S8R element			
10 × 10	0.02405(540) ABAQUS S4R element			
1 × 1	0.02441(110) $p = 8$ by p-version			

Figures in parentheses give *NDOF*.

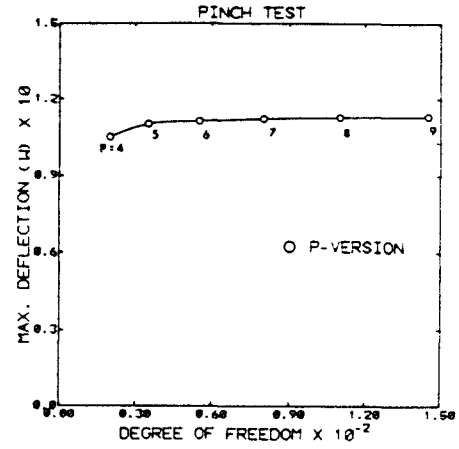

Fig. 4. Convergence of p-level and $NDOF$ vs w (max).

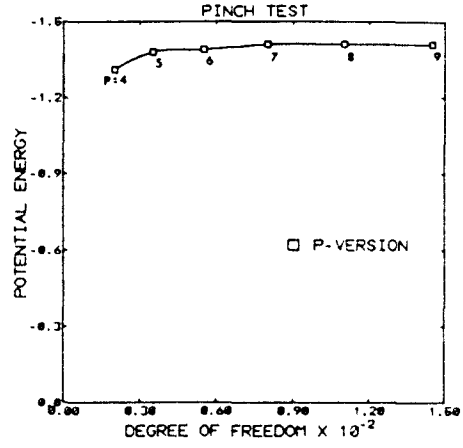

Fig. 5. Convergence of $NDOF$ vs potential energy.

based on the [10 × 10] S4R model and 26.69 s by the [5 × 5] S8R element. These runs were made on a VAX-8800 computer. It is expected that more spectacular savings in CPU time can be achieved with the p-version if a more efficient equation solver and quadrature algorithm are used. It is worthwhile to note that to achieve the same level of accuracy, a single fifth-order element requires 13.86 s of CPU time whereas 49 quadratic elements require 65.77 s of CPU time when both runs are made with SHLPV.

4.2. *Lockheed test problem 2*

A problem with a cylindrical shell with two symmetrically located rectangular cutouts, subjected to axial displacement, was solved. This problem was chosen because of the high quality of the elements used and the availability of well-documented solutions by means of other computer codes (Szabo *et al.*, 1976; Rossow *et al.*, 1975).

The most challenging aspect of this problem is that the re-entrant corners of the cutout are singular points, that is, an elastic analysis will give infinite stresses at these points. The question is whether approximations based on a few high order p-version finite elements can perform as well as approximations based on a large number of lower order conventional

Table 4. Results of mesh refinement with $p = 5$

Number of mesh elements	$NDOF$	P.E.	W_{max} (in.)
1	34	−0.138E+1	0.110131
2	70	−0.139E+1	0.111125
4	125	−0.142E+1	0.113417

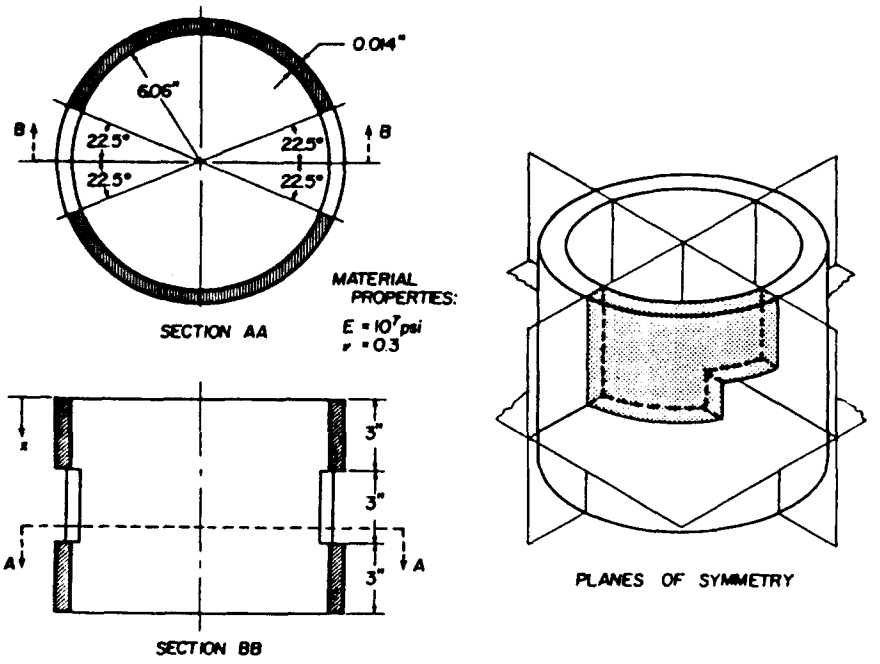

Fig. 6. Cylinder with cutouts (Szabo *et al.*, 1976).

finite elements in representing the state of stress in the neighborhood of the re-entrant corners.

The details of the problem, known as "Lockheed test problem 2" are shown in Fig. 6. The boundary conditions at the ends of the shell are $v = w = \theta_x = \theta_y = 0$ and $u = \text{const.} = 0.2 \times 10^{-3}$ in. Because of symmetry, only one octant of the structure has to be modeled. The problem was solved with the program SHLPV by increasing the number of elements from 3 to 5 when $p = 9$. The solution appeared to converge with $p = 9$ and a three-element mesh, as shown in Fig. 7.

In Figs 7–12, the results of the p-version are compared with those of the program TRISHL developed by the National Aeronautical Establishment of Canada and the Constraint Method program developed at Washington University.

The five-element SHLPV mesh used in the analysis of the problem is inset in Figs 7–12. The 100-element TRISHL mesh and the ten-element Constraint Method mesh are shown in Fig. 13. In Table 5, a comparison is provided of the number of elements and the degrees of freedom used in the application of several computer programs to the test problem.

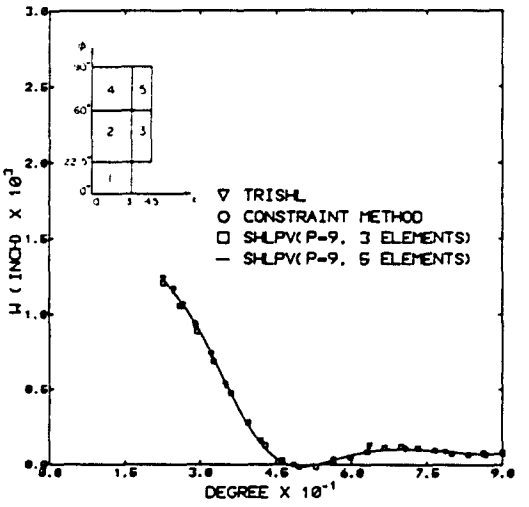

Fig. 7. Normal displacement along centerline of shell ($x = 4.5$ in.).

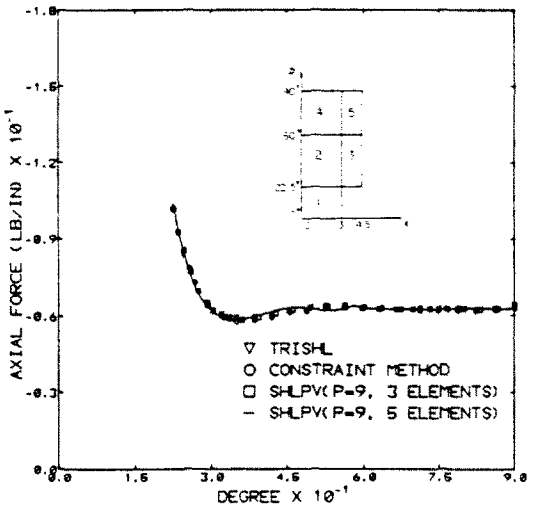

Fig. 8. Axial normal force distribution along centerline of shell.

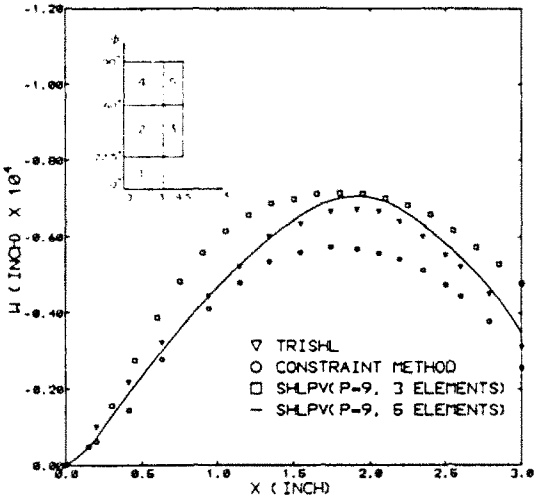

Fig. 9. Normal displacement along axial line, $\theta = 0$.

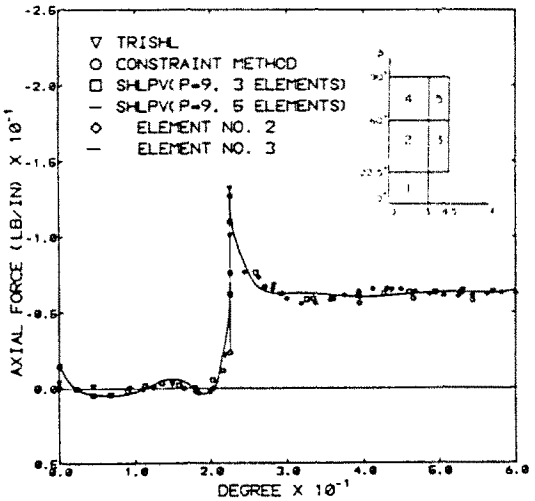

Fig. 10. Axial normal force distribution at $x = 3$ in.

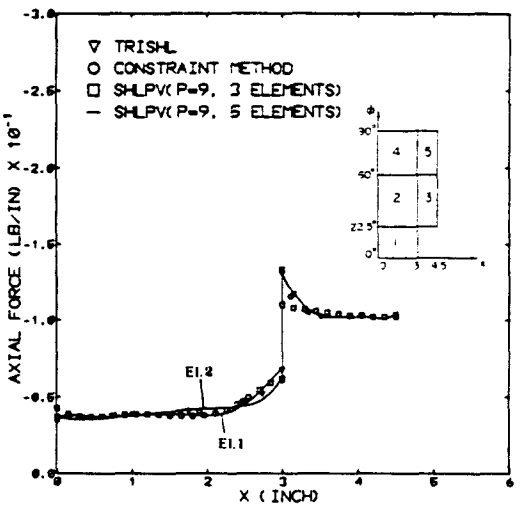

Fig. 11. Axial normal force distribution at $\theta = 22.5^\circ$.

Particular mention should be made of the drastic reduction in the number of finite elements (three elements) required by the p-version program, SHLPV. The required number of elements reported in the published literature ranged from 10 to 476 and the *NDOF* from 500 to 2457. The three-element (*NDOF* = 340) SHLPV model gave very good approximations of both deflections and stresses. Moreover, the CPU time required was found to be highly competitive with those reported by others.

The greatest discrepancies appearing between the Constraint Method, TRISHL, and SHLPV results are shown in Fig. 9. The magnitude of the displacements by the Constraint Method shown in this figure are, however, relatively small, actually more than two orders of magnitude smaller than the largest computed displacement. The results of SHLPV appear to agree more closely with those of TRISHL. In Figs 10–12, the axial forces and bending moments existing in the shell in the vicinity of the re-entrant corner are shown. It may be noted that multi-valued stress predictions are shown for the re-entrant corner, depending upon the element being considered.

Since the SHLPV program is based on shear deformation theory, the normal displacements are a little larger than those by TRISHL and the Constraint Method. The bending moments agree very well everywhere including the re-entrant corner.

4.3. *Elastic through-wall cracked cylinder*

Figure 14 shows a cylinder containing a circumferential through-wall crack with a total included angle of 2θ, R being the mean radius and t the wall thickness. The crack length

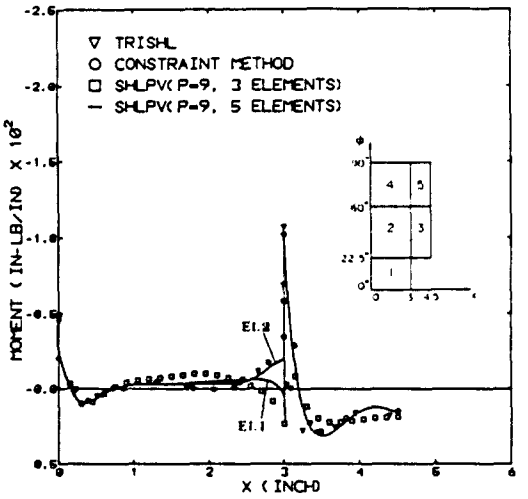

Fig. 12. Axial bending moments at $\theta = 22.5^\circ$.

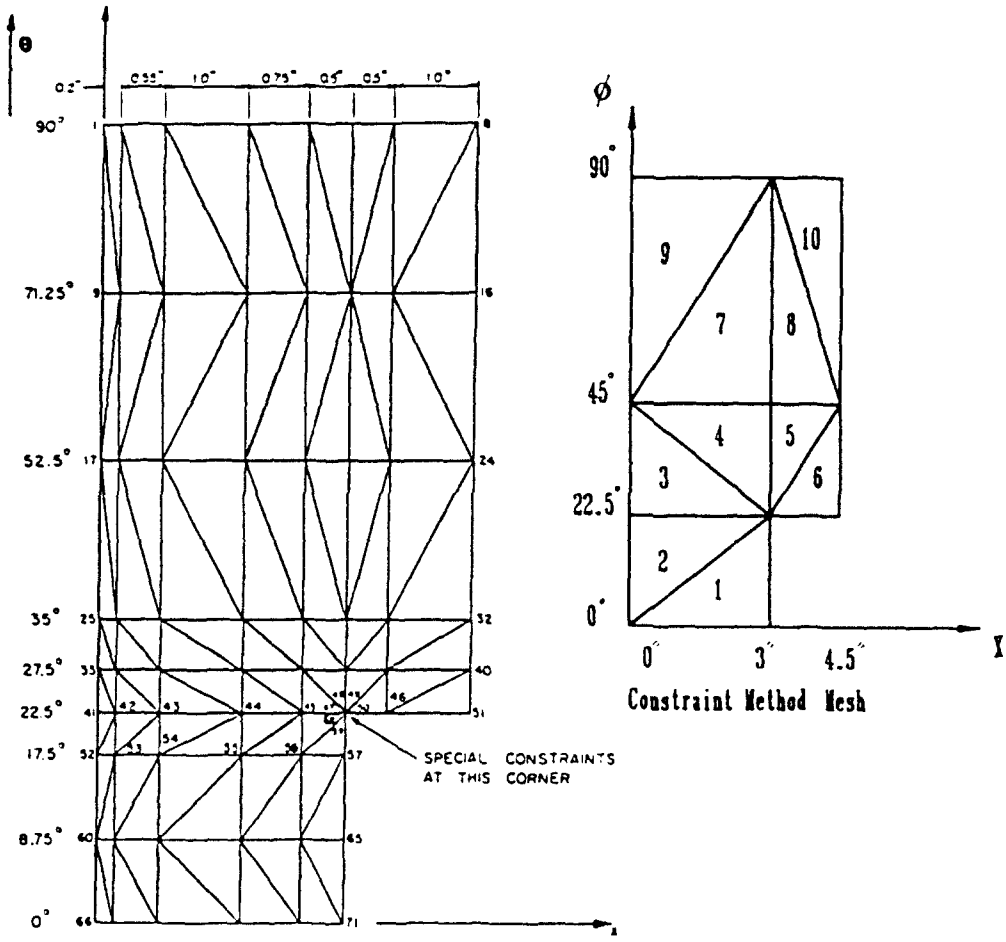

Fig. 13. One hundred-element TRISHL mesh and ten-element Constraint Method mesh (Rossow *et al.*, 1975).

$(2a)$ in the circumferential direction is then $2\theta R$. The loading is considered to be due to a remotely applied axial tensile force P. The Virtual Crack Extension Method was employed to calculate the stress intensity factor, K, using the relationship: $G = K^2/E$, where G is the energy release rate. E was taken to be 0.2×10^6 psi, $R = 30$ in. and Poisson's ratio $\nu = 0.3$. For cylinders under tension loading, K can be expressed as

$$K = \frac{P}{2\pi Rt}\sqrt{(\pi a)}F(\theta, R/t, \nu). \tag{10}$$

Parameter F is variously described as the shape factor, the non-dimensional geometric dependent coefficient of the stress intensity factor or the geometrical magnification factor.

Table 5. Lockheed test problem 2: comparison of key computational parameters

Computer code	Source references	Number of elements	Degrees of freedom
SHELL 9	Gulf General Atomic, Inc.	476	2457
STAGS	Lockheed Missiles & Space Corp.	342	1437
REXBAT	Lockheed Missiles & Space Corp.	241	1125
TRISHL	National Aeronautical Establishment, Canada	100	637
Constraint method	Washington University	10	500 (6 6 7 case)
SHLPV p-version	Vanderbilt University	3	340 ($p = 9$)

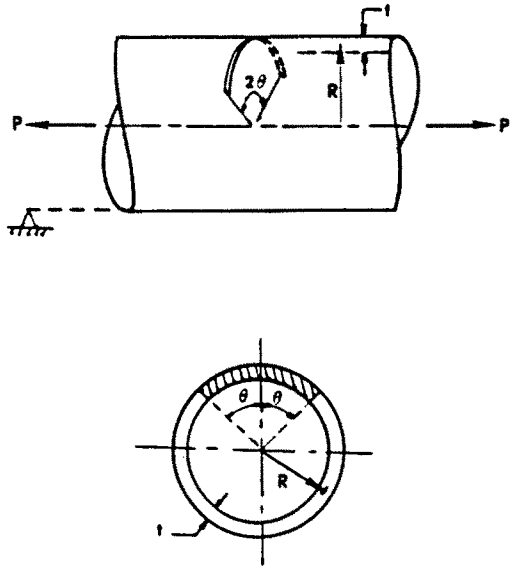

Fig. 14. Through-wall cracked cylinder under tension.

The value of K for a fairly broad range of values of θ and R/t with $\nu = 0.3$ have been presented by Folias (1967), Erdogan and Delale (1979), Sanders (1982), Kumar *et al.* (1984), and Zahoor (1985) using different methods. For $R/t = 10$ and $2\theta = 90^\circ$, the SHLPV model with $p = 8$, and four elements gives $F = 1.74020$, which is in excellent agreement with the F value of 1.72656 obtained using the short crack expression of Sanders (1982). For $R/t = 5$ and $2\theta = 90^\circ$, the F value computed by the same SHLPV model is 1.52953 which again is in very good agreement with the result of 1.56254 obtained by Zahoor (1985). The third case examined corresponds to $R/t = 20$ and $2\theta = 90^\circ$. In this case the same SHLPV model as above gives $F = 2.10615$, which compares very well again with the solution of 2.07495 obtained by Zahoor (1985) and the solution of 1.974 obtained by Kumar *et al.* (1984). Monotonic convergence of the shape factor, F, as the p-level with a four-element SHLPV model is increased from 1 to 8 is shown in Fig. 15. Figure 16 shows the excellent agreement of F values for different crack lengths obtained by SHLPV and those by Sanders (1982) and Zahoor (1985).

In obtaining the value of K Kumar *et al.* (1984) used the software ADINA. The finite element model consisted of 242 nine-noded thin shell elements and 989 nodes. On the other hand to achieve the same degree of accuracy, SHLPV required only four eighth-order elements involving 153 nodes and 555 degrees of freedom.

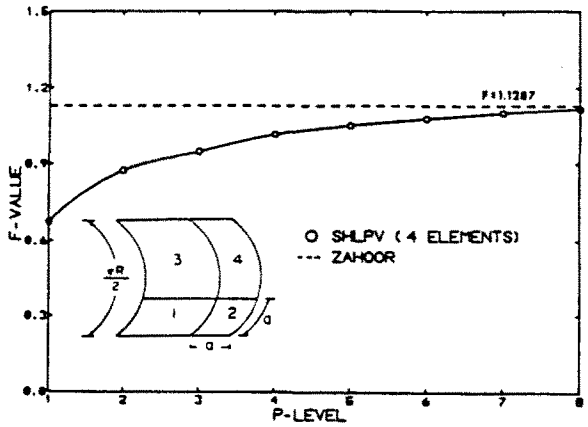

Fig. 15. Values of F with different p-levels ($R/t = 10$, $2\theta = 30^\circ$).

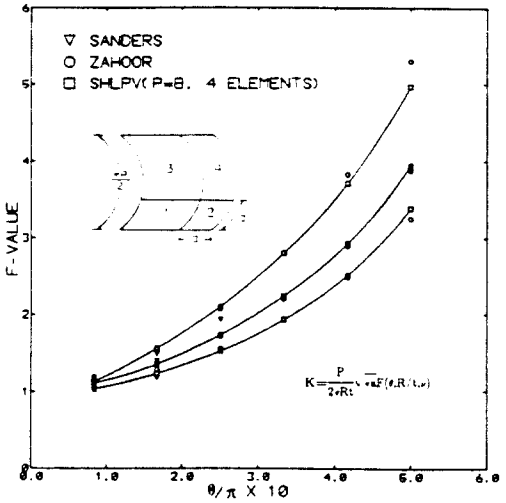

Fig. 16. Comparison of elastic solutions for a through-wall cracked cylinder under tension: $R/t = 5$, 10, 20.

5. CONCLUSIONS

Hierarchic shell elements of high order using exact blend mapping satisfies all the requirements of constant strain states and rigid-body modes. The stiffness matrix based on the proposed element is well conditioned even when very high levels of p are used.

In the case of the pinched shell test problem, modeling of one octant of the shell with just one element of ninth order leads to a very accurate value for maximum deflection (0.113 in.). Although a graded model consisting of four fifth-order elements leads to a slightly better value for the maximum deflection (0.1134 in.), the SHLPV models are found to be computationally more efficient than ABAQUS models.

In the case of the Lockheed test problem, the proposed p-version elements proved to be very efficient both in terms of accuracy and computational efficiency. To achieve the same order of accuracy in displacements and stresses, the problem was solved with three and five p-version elements as compared to ten elements by the Constraint Method and 100 elements by TRISHL.

In the case of the cracked shell problem it is found that reliable values of the stress intensity factor can be obtained with only a four-element model.

The proposed p-version shell element is therefore a worthy alternative to the existing cylindrical shell elements.

Acknowledgement—The work presented in this paper was partly supported by NSF Grant No. CEE-84115675 and partly by the computing resources of NSF Grant No. MSM-8704649.

REFERENCES

Ashwell, D. G. and Gallagher, R. H. (1976). *Finite Elements for Thin Shells and Curved Members*. Wiley, New York.

Basu, P. K. (1986). Dimensional reduction of structural plates and shells. NSF Research Report, Grant No. CEE-84115675, Vaderbilt University, Nashville, Tennessee.

Basu, P. K. and Lamprecht, R. M. (1979). Some trends in computerized stress analysis. *Proc. Seventh A.S.C.E. Conf. on Electronic Computation*, Washington University, St. Louis, Missouri.

Basu, P. K. and Peano, A. G. (1981). Adaptivity in p-version F.E. approximation. A.S.C.E., Preprint 81-527, St. Louis, Missouri.

Basu, P. K., Rossow, M. P. and Szabo, B. A. (1977). Technical Documentation and User's Manual: COMET-X. Report No. R-340, Federal Railroad Administration.

Bogner, F. K., Fox, R. L. and Schmit, L. A. (1967). A cylindrical shell discrete element. *AIAA J.* **5**, 745.

Cantin, G. (1970). Rigid body motions in curved finite elements. *AIAA J.* **8**, 1252.

Cantin, G. and Clough, R. W. (1968). A curved cylindrical shell, finite element. *AIAA J.* **6**(6), 1057–1062.

Carpenter, N., Stolarski, H. and Belytschko, T. (1986). Improvement in 3-node triangular shell elements. *Int. J. Numer. Meth. Engng* **23**, 1643–1667.

Cheng, C. (1986). Dynamic analysis by the p-version of the finite element method. Ph.D. Dissertation, Purdue University.

Erdogan, F. and Delale, F. (1979). Transverse shear effect in a circumferentially cracked cylindrical shell. *Q. Appl. Mech.* **37**, 239–258.

Folias, E. S. (1967). A circumferential crack in a pressurized cylindrical shell. *Int. J. Fracture Mech.* **3**, 1–11.

Gordon, W. J. (1971). Blending function methods of bivariate and multivariate interpolation and approximation. *SIAM J. Numer. Analysis* **8**(1), 158–177.

Hansen, J. S. and Heppler, G. R. (1985). A Mindlin shell element that satisfies rigid-body requirements. *AIAA J.* **23**(2), 288–295.

Hibbitt, Karlsson and Sorensen, Inc. (1985). ABAQUS Example Problems Manual.

Kumar, V., German, M. D., Wilkening, W. W., deLorenzi, H. G. and Mowbray, D. F. (1984). Advances in elastic–plastic fracture mechanics. NP-3607 Research Project 1237-1, prepared by General Electric Company for E.P.R.I.

Lukasiewicz, S. A. (1976). Introduction of concentrated loads in plates and shells. *Prog. Aerospace Sci.* **17**(2), 109–146.

Peano, A. G., Szabo, B. A. and Metha, A. K. (1978). Self-adaptive finite elements in fracture mechanics. *Comp. Meth. Appl. Mech. Engng* **16**, 69–80.

Rossow, M. P., Lee, J. C. and Chen, K. C. (1975). Computer implementation of the Constraint Method. Report DOT-OS-30108-3.

Sabir, A. B. and Lock, A. C. (1972). A curved cylindrical shell finite element. *Int. J. Mech. Sci.* **14**, 125–135.

Sanders, J. L. Jr. (1982). Circumferential through-cracks in cylindrical shells under tension. *J. Appl. Mech.* **49**, 103–107.

Szabo, B. A., Peano, A. G., Katz, I. N. and Rossow, M. P. (1976). Advanced finite element technology for stress analysis. Report DOT-TST-76-71.

Thomas, G. R. and Gallagher, R. H. (1975). A triangular thin shell finite element: linear analysis. NASA CR 2482.

Timoshenko, S. P. and Woinowsky-Krieger, S. (1959). *Theory of Plates and Shells*, 2nd Edn. McGraw-Hill, New York.

Zahoor, A. (1985). Closed form expressions for fracture mechanics analysis of cracked pipes. *J. Pressure Vessel Technol.* **107**, 203–205.